

Optical Fibers and Cavities

Shashank Dharanibalan^{a)}

In this second lab investigation, we've managed to construct an optical system with a Keplerian telescope to reduce the beam waist of a Gaussian beam of a He-Ne laser to couple into a Multi-Mode optical fiber with $63.3 \pm 3.7\%$ coupling efficiency and then into a Single-Mode optical fiber with $3.12 \pm 5.23\%$ coupling efficiency. The coupling efficiency of the SM mode over the MM mode is $5.44 \pm 9.34\%$. The second part of the lab involved the creation of a bow-tie optical cavity with a concave mirror and back-polished mirrors to observe the resonance of a laser beam in various TEM modes of Hermite-Gaussian and Laguerre-Gaussian polynomials. The inclusion of a specific lens system before the cavity to match the q-parameter of the cavity results in matching the mode to Hermite-Gaussian mode 0,0.

Keywords: Optical Fiber, SM mode, MM mode, Coupling, Resonance, Optical cavity

I. INTRODUCTION: OPTICAL FIBERS

II. THEORY

The coupling of an optical fiber requires the understanding of how a light beam propagates with Gaussian wavefronts through an optical system and how the design of an optical fiber allows light to pass through the fiber.

II.A. Gaussian Beam

The wavelike properties of a light beam can be seen in the behavior of its electric field after the paraxial approximation that gives the transverse profile of the light beam as it propagates in the \hat{z} direction. [1]

$$E = \xi_0 \frac{\omega_0}{\omega(z)} e^{-i\phi z} e^{ik \frac{x^2+y^2}{R(z)}} e^{i(kz - \omega t)} \quad (1)$$

Where $R(z)$ and $\omega(z)$ are the radius of curvature of the wavefront and the beam waist of the light beam which can be stored in the handy q-parameter seen in Eqn. 2 that defines the profile of the beam at a given point as the beam propagates.

$$\frac{1}{q} = \frac{1}{R(z)} - i \frac{1}{\pi \lambda(\omega(z))^2} \quad (2)$$

The beam profile changes as it propagates some free distance as the radius of curvature decreases and the beam waist increases as the beam diverges. The effect of a free space distance (L) propagated by the beam can be calculated linearly.

$$q_1 = q_0 + L \quad (3)$$

II.B. Gaussian Beam in optical systems

When an optical component is involved the beam profile can be altered to maintain or reduce the beam waist, such as a lens that reduces the beam waist based on the

focal length of the lens. The q-parameter after an optical component can be derived algebraically, where A,B,C, and D are the elements of a matrix that represents the effect of a general optical component.

$$q_1 = \frac{Aq_0 + B}{Cq_0 + D} \quad (4)$$

The ABCD matrix, as they are called, for a thin lens of focal length (f) and for a free space propagation of distance (L) are as follows

$$M_{\text{lens}} = \begin{pmatrix} 1 & 0 \\ -\frac{1}{f} & 1 \end{pmatrix}, M_{\text{free}} = \begin{pmatrix} 1 & L \\ 0 & 1 \end{pmatrix} \quad (5)$$

II.C. Optical Fiber

An optical fiber is a tube that allows it to losslessly transmit from one end to another end via total internal reflection. The design of an optical fiber consists of two layers with different indices of refraction. The first outer layer is called the cladding layer and it has a lower index of refraction than the inner core layer with a radius a . The cladding layer constrains the light to remain in the core layer. The condition of coupling for total internal reflection comes from the application of Snell's law to the two indices of refraction.[2]

$$\sin \frac{\theta_c}{2} = \sqrt{(n_0^2 - n_{\text{clad}}^2)} \quad (6)$$

This is referred to as the *numerical aperture* or NA. For multi-mode fiber, it can accommodate many modes which can be calculated as the maximum number of modes in the fiber from the V-parameter.

$$V = \frac{2\pi a}{\lambda} \sqrt{(n_0^2 - n_{\text{clad}}^2)} \quad (7)$$

III. PROCEDURE

We set up an optical system to pass a Gaussian beam of the laser through two thin lenses with appropriate distances to be optimized to be incident with the smallest beam waist on the collimator. A collimator is an aspheric lens with a small enough focal length and on kinematic mounts to align the beam into an optical cable through a connector.

III.A. Simulation of lens set-up

Before the hands-on experiment is carried out, a simulation of the propagation is done through individual ABCD matrices multiplied to form a composite matrix that represents the entirety of the optical system. The goal of the simulation is to optimize the position of the lenses so the beam waist after the optical system matches the target beam waist on the collimator so the optical fiber can be coupled easily.

Eqn 5 gives the building blocks for the system we are constructing in a simulation, using two chosen focal lengths, the following gives the composite matrix for our optical system.

$$\begin{pmatrix} 1 & L_c \\ 0 & 1 \end{pmatrix} \begin{pmatrix} 1 & 0 \\ -\frac{1}{f_2} & 1 \end{pmatrix} \begin{pmatrix} 1 & L_b \\ 0 & 1 \end{pmatrix} \begin{pmatrix} 1 & 0 \\ -\frac{1}{f_1} & 1 \end{pmatrix} \begin{pmatrix} 1 & L_a \\ 0 & 1 \end{pmatrix} = \begin{pmatrix} A & B \\ C & D \end{pmatrix}$$

The actual simulation to find the q-parameter is seen in the appendix. There is no singular solution even with reduced degrees of freedom so an optimization process needs to be conducted for the program to print out lengths between the laser and the first lens and second lens before we set the apparatus in the laboratory.

III.B. Beam set-up into collimator

For the calculation of the beam waist incident on the collimator, we can treat the collimator to the fiber as a trigonometric calculation that allows us to use the NA formula from Equation 6. Where f_3 is the focal length of the collimator (the third lens in the set-up) and ω_{coll} is the beam waist we want the lens system to match on the collimator.

$$\text{NA} = \sin \theta = \frac{\omega_{\text{coll}}}{\sqrt{\omega_{\text{coll}}^2 + f_3^2}} \quad (8)$$

$$\omega_{\text{coll}} \approx \text{NA} * f_3 \quad (9)$$

III.C. Alignment for maximum coupling

With the target beam waist calculated and the simulation run, the optimized set-up of the apparatus and all the distances can be seen in Fig 1. The optimization algorithm in the first subsection of the Appendix gives L_a to be 44 cm and L_b to be 18 cm.

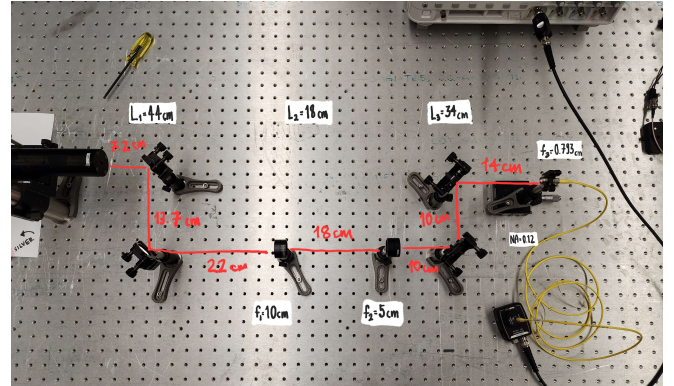


FIG. 1: L_a represents the distance from the first beam-steering mirror to the first lens and L_b is the distance between the two lenses. The total path covered by the laser is 61 cm

The two sets of beam-steering mirrors downstream help further align the input beam on the collimator after beam waist reduction. The centering of the beam on the collimator by these mirrors was easy as the beam waist was small enough to see the effects of the smallest movements of the mirror adjustments. However, the kinematic mount of the collimator adjusted with a screwdriver in small increments allows for more minute control of the alignment. The most reliable way to check for alignment is maximizing the reading on the oscilloscope by feeding the other end of the optical fiber through a 'narrow key' focused on the photodetector. Judging the brightness of the light out of an optical cable by eye in a dark room is less reliable than an RMS Voltage reading by the sensitive photodetector.

The alignment settings described from the simulation are ideal for the SM fiber but we first connect the MM fiber as the core diameter is larger and thus more forgiving for alignment. It makes it easier to slowly perfect the coupling for the MM fiber and then with the SM fiber with the narrower core. The goal for both coupled fibers is to measure the RMS Voltage for different terminator settings with multiple trials. The optical coupling efficiency would be the ratio of the RMS voltage after the fiber over the RMS voltage before the lens system. Additionally, we passed the light through the narrow key into a polarizing beam splitter and observed the RMS Voltage between two photodetectors.

IV. TABULATED RESULTS

The tabulated data results for each terminator setting are an average for multiple trials and it is evidence that the Input RMS Voltage and the RMS Voltage measured with coupled MM fiber reach saturation where the current generated by the photodetector crosses the threshold that the oscilloscope can output.

Terminator ($k\Omega$)	Input RMS (V)	MM RMS (V)	SM RMS (V)
1	0.84	0.4725	0.114
5	4.2	2.7	0.024
10	8.2	5.4	0.039
50	9.3	9.3	0.72
100	9.5	9.5	1.74

TABLE I: This table contains the voltage readings from the photodetector at different terminator settings, this is because the readings at a single terminator resistance setting can be unreliable.

V. DATA RESULTS

V.A. Extrapolation to ideal case

However, it is at the higher terminator settings where the coupled SM fiber has stable and low errors in RMS Voltage. The goal is to extrapolate the values for the Input and coupled MM Fiber linearly to obtain and compare the optical coupling for the MM Fiber at $100 k\Omega$ to the SM Fiber at the same setting.

Figure 2 shows the saturated and ideal linearly fitted plot of the RMS voltage for the multi-mode fiber and input laser. The linear fit comes from our expectation that Ohm's law holds for the photodetector.

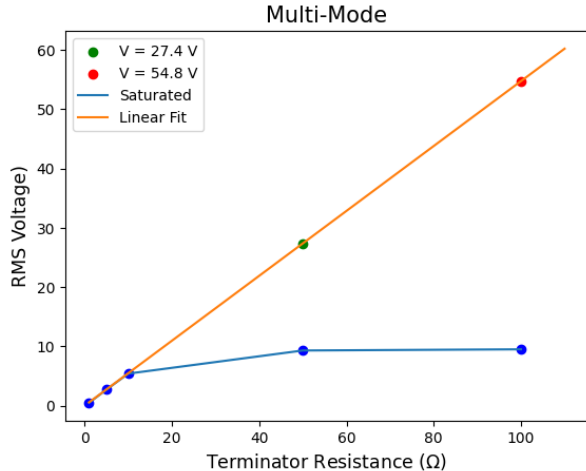


FIG. 2: The saturated and the extrapolated RMS voltage for the MM fiber by a linear fit.

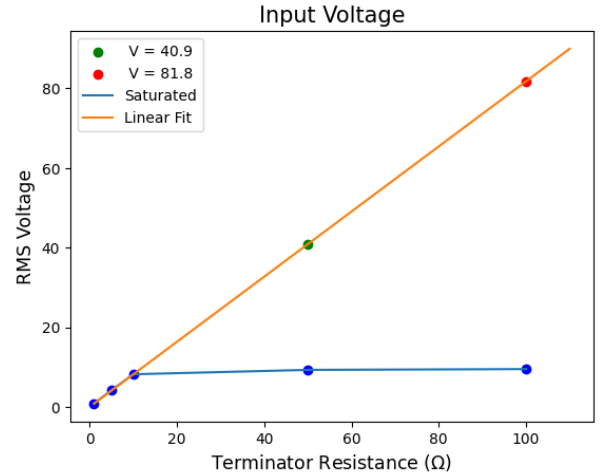


FIG. 3: The saturated and extrapolated RMS voltage for the input laser by a linear fit.

V.B. Coupling efficiencies

The newly found extrapolated data can be used now to calculate the optical coupling efficiency for each fiber and then the ratio to get the efficiency ratio between the fibers. The mean of the calculations across all the terminator settings and the standard deviation of the calculations give coupling efficiency and the errors associated.

Fiber	Coupling Efficiency
MM	57.89 ± 0.04 (%)
SM	1.9 ± 0.02 (%)
SM/MM	0.03 ± 0.02

TABLE II: The calculated coupling efficiency and efficiency ratio. The efficiency is averaged calculations and the standard deviation gives the error on the efficiency

V.C. Behavior of light through a PBS

The data was displayed onto an oscilloscope where light exiting the optical fiber was split into the transmission channel and reflected channel. When the fiber was gently shaken or air was blown over it, the power output for both channels changed between a maximum and minimum for each laser beam photodetector. The dynamic voltage is because the light entering the PBS is polarized and the condition of total internal reflection for all polarization orientations changes when the fiber is moved even slightly. Each photodetector detects a particular polarization and the amount of light that is transmitted in that polarization orientation changes.

V.D. Error Analysis

The target beam waist calculation as seen in Equation 9 and expounded in the Appendix was just the upper

limit of the beam waist that the collimator can take and focus into the optical fiber, while the simulation we ran produced a minimum beam waist that is smaller than the target beam waist. However, it makes it harder for alignment as the entering beam waist is already very small. The alignment for the MM fiber was easier as the lens system was already set up for an SM fiber and the larger core diameter than the entering waist of the laser in the MM fiber meant better coupling compared to the single-mode.

Additionally, the translation of the simulated lengths onto the actual lab mounting table is not perfect and the small changes of a couple of millimeters can change the beam waist by an order of magnitude of 4-5x. The distances were verified via a ruler and are not exactly the distances covered by the laser as it may take a slightly longer path if it does not hit the center of each beam-steering mirror. Although the target beam waist is large enough to allow leeway, the alignment process on the SM fiber could be flawed. Furthermore, the handling of the SM fiber whilst aligning could result in alignment errors. The use of a moving mounting plate was helpful for alignment but as another degree of freedom, it could restrict us from getting even better alignment.

VI. CONCLUSION

The coupling efficiency of the Single Mode fiber is drastically lower than the theoretical expectation due to the inability to exactly transform the optimized solution from the ABCD simulation of the lens, compounding path length differences of the laser beam before arriving at the collimator and the incomplete centering and alignment of the input laser due to the moveable mounting plate. Additionally, the optimized solution is one of many and it is possible we would have had better chances with another solution with more room for the beam-steering mirrors downstream and a shorter total path length so the laser beam doesn't diverge too much.

VII. INTRODUCTION: OPTICAL CAVITIES

VIII. THEORY

VIII.A. A stable bow-tie optical cavity cavity

A bowtie optical cavity is as the name suggests, an optical cavity that is shaped like a bow-tie to capture light in a volume. The design is flexible to allow the cavity to be small and fit on a vibration-absorbent breadboard. The light beam enters through the input mirror and is reflected across the diagonal of the cavity by the second mirror to a concave mirror that reduces the beam waist and is reflected by the third mirror that reflects back the other diagonal onto the first mirror to complete a trip around the total path of the optical path. [3]

VIII.B. Simulation of a cavity

An optical cavity, similar to the optical fiber has a composite ABCD matrix system that simulates the path of the light beam through the cavity and the construction of a stability cavity depends on the length and width as seen by the ABCD matrices.

$$\begin{pmatrix} 1 & L+D \\ 0 & 1 \end{pmatrix} \begin{pmatrix} 1 & 0 \\ \frac{-1}{f_3} & 1 \end{pmatrix} \begin{pmatrix} 1 & D+L \\ 0 & 1 \end{pmatrix} = \begin{pmatrix} A & B \\ C & D \end{pmatrix}$$

VIII.C. q-parameter of an optical cavity

A stable cavity is when the path covered by the light beam from the first input mirror to the concave mirror and from the concave mirror and back to the input mirror is equal. The stable cavity has an ABCD matrix construction whose imaginary part is greater than 0 but less than 1 as A,B,C, and D are real.

$$\begin{aligned} q_{\text{res}} &= \frac{Aq_{\text{res}} + B}{Cq_{\text{res}} + D} \\ q_{\text{res}} &= \frac{A - D\sqrt{(A + D)^2 - 4}}{2C} \\ 0 \leq \frac{(A + D)^2}{4} &\leq 1 \end{aligned}$$

VIII.D. Mode-matching with a telescope

The path of the light beam can take many trips and the behavior of the light in the cavity is similar to a harmonic oscillator and the greater the oscillations, the higher the frequency, and the state is in a different quantized state. Similarly, the cavity is separated by different discrete modes based on the path length covered by the light beam and the resonance in the cavity. Thus, a telescope can be added to the set-up, like for an optical fiber, to match the q-parameter of the cavity and help display on the lowest mode called TEM_{0,0}. Therefore, using the same function set-up to simulate a telescope for optical fibers, we can set a new optimization process to match the resonance q-parameter of the cavity

$$\frac{1}{q_{\text{res}}} = \frac{D - A}{2B} - i \frac{\sqrt{4 - (A + D)^2}}{2B} \quad (10)$$

IX. PROCEDURE FOR CAVITY-BUILDING

IX.A. Simulation choices before building

The cavity building can begin after a successful simulation is conducted to check for resonance and stability of a particular choice of cavity. The cavity is to rest on an optical breadboard so it was convenient to choose a rectangular cavity in inches and the simulation code seen in the second Appendix highlights the check for stability

using the matrix conditions derived for a stable cavity in Equation 10

The mirror choices are two back-polished mirrors as the input and the output mirrors so light can not only enter the cavity but also exit the cavity after resonating through multiple paths around the cavity mirror. The concave mirror with a positive radius of curvature reduces the beam waist within the cavity and a regular planar focal mirror is driven by a PZT for better observation of resonance. Figure 2 shows the setup for the optical cavity without mode-matching.

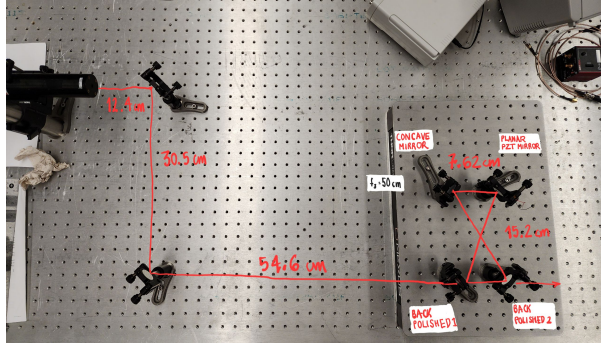


FIG. 4: The back-polished mirror has a non-zero transmissivity allowing light to enter and leave the cavity acting as the input and output mirrors. The focal length of the concave mirror is half the radius of curvature

IX.B. Alignment within the optical cavity

The lengths for the cavity are doubly verified using a piece of string to measure distances and for ease of use, the stable cavity choices allow for the mirrors to be placed in the center of the equally spaced mounting holes on the optical breadboard. The mirrors outside the cavity system were placed on higher mounts to account for the height of the breadboard and level the beam entering the cavity. Additionally, it allowed for space to be left for a mode-matching lens system.

To begin alignment, the input laser was aligned without the presence of the input back-polished mirror. The input beam could be seen clearly in a lit lab room easily and it was used to best align the beam on the center of the second/output mirror and beam-walked to the center of the third/concave mirror and finally on the regular plano-focal mirror with care because the concave mirror's positive curvature results in large changes in beam direction for small adjustments. The concave mirror is not be adjusted after.

To prepare to "close" the cavity with the first/input mirror, a transparent ruler can be held perfectly vertically on the location of the input mirror's mount to align the final/fourth planar mirror reflected beam to the loca-

tion of the input beam from the laser. With the lights off, the input mirror post is slotted back into the mount and aligned until light can be dimly seen on the second mirror. The misalignment of the input mirror will be apparent as the beam will no longer be a singular dot. The misalignment compounds with each path around the cavity resulting in multiple spots. To put it rudimentarily, the goal is to collect all these reflected dots as close together as possible in the center of the mirror, only using the newly mounted input mirror and the planar mirror. The closest alignment that we got was a square of reflections that flickered spasmodically as alignment improved.

IX.C. Resonance observation and mode visualization

The resonance can be observed if the photodetector beyond the second input receives an output laser beam but also if the planar beam is driven by a PZT (Piezo electric transducer), the resonance can be controlled by the transducer as it varies the total path of the circuit by a few microns depending on the driving frequency and the voltage supplied to the transducer. This helps observe the linewidth, the standard deviation from the peak voltage, and the finesse which is the sharpness of the peaks on the oscilloscope with voltage as a function of the voltage ramp of the PZT transducer.

IX.D. Mode-matching with a lens system

The ample space provided should allow for easy insertion of the lens system into the space between the beam-steering mirrors and optical breadboard. The optimized code accounts for this space and parameterizes the distances to be calculated for the q-parameter of the telescope to match the q-parameter of the cavity. Figure 4 shows the full setup within the original cavity setup

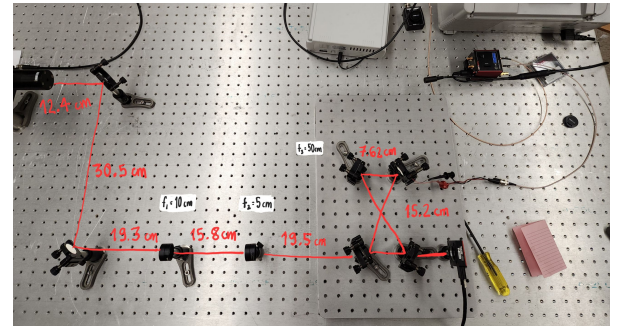


FIG. 5: The two lenses for this system are the same as the optical fiber system but the optimization sets new distances to match the q-parameter of the optical cavity

X. RESULTS

The oscilloscope outputs the Voltage as a function of the input voltage from the transducer, where the function generated is a triangle wave with a low driving frequency of around 2 Hz, to begin with to observe the modes.

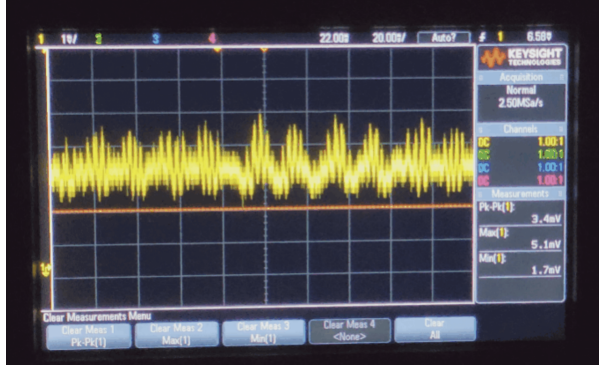


FIG. 6: The resonance of the cavity driven by a triangle wave function with a driving frequency of 2 Hz on the PZT

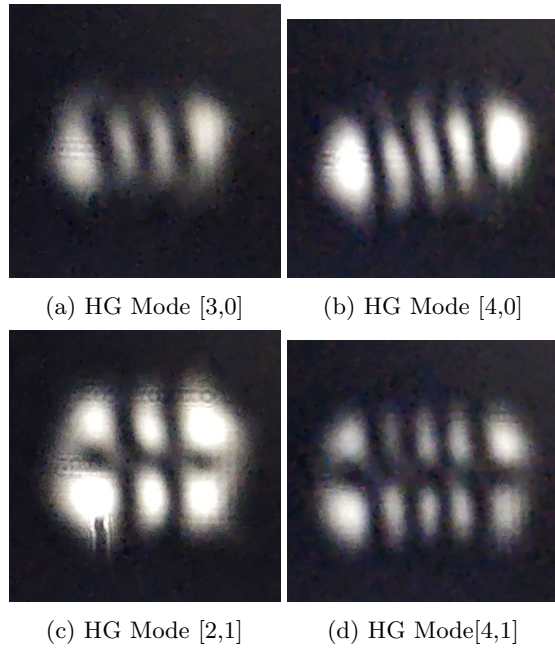


FIG. 7: Lower Modes at the same driving frequency, the image a) is the brightest and is most frequently seen compared to the other four when mode-matched.

After mode-matching the lower modes were still visible but the lowest TEM mode as seen in Figure 7a became the brightest and was visible for longer on the camera before oscillating to the higher modes and back

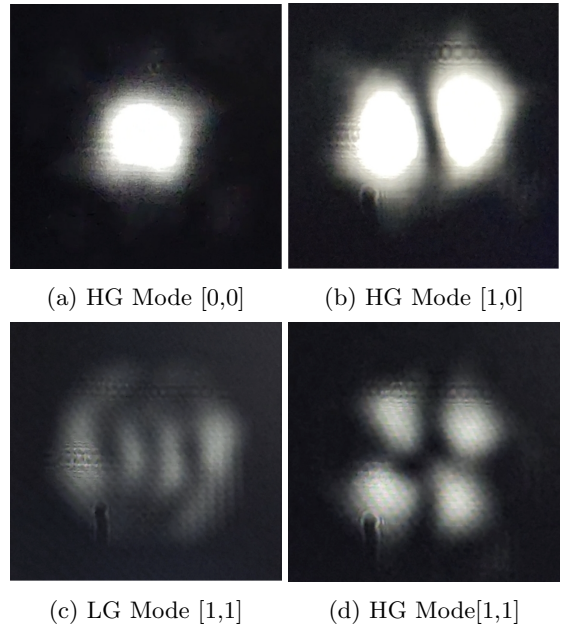


FIG. 8: Lower Modes at the same driving frequency, the image a) is the brightest and is most frequently seen compared to the other four when mode-matched.

The reason the lowest TEM mode alone wasn't visible was because the function generator and driving frequency were constant and employing a feedback loop would help hold the resonance in the lowest mode so only the $\text{TEM}_{[0,0]}$ would be visible. A feedback loop would vary the frequency so the oscillations would be more regular with the same voltage peaks and troughs on the oscilloscope. This would mean that the linewidth and the finesse would be constant.

XI. CONCLUSION

The stable optical cavity results in resonance when the trapped light enters the cavity and makes multiple trips around the cavity behaving like a harmonic oscillator. The light in the cavity can be seen flickering and the photodetector picks up resonance when a driving frequency and a voltage ramp are applied. Additionally, for a lens system that matches the q-parameter of the lens telescope with the q-parameter of the cavity, the lowest modes are only visible with $\text{TEM}_{[0,0]}$ being the brightest. The most reliable way to display on the lowest TEM mode is to set up a feedback loop to alter the driving frequency and voltage ramp.

Appendix A: Target beam waist and theoretical coupling calculation

Insert the diagram showing the trigonometry reduction, use that to calculate the NA of the lens, and com-

pare it to the NA of the fiber.

$$\text{NA} = \sin \theta = \frac{\omega}{\sqrt{\omega^2 + f^2}}$$

$$\text{NA}^2 \omega^2 + f^2 = \omega^2$$

$$f^2 = \frac{\omega^2 (1 - \text{NA}^2)}{\text{NA}^2}$$

$$f^2 \approx \frac{\omega^2}{\text{NA}^2}$$

$$\omega = f * \text{NA}$$

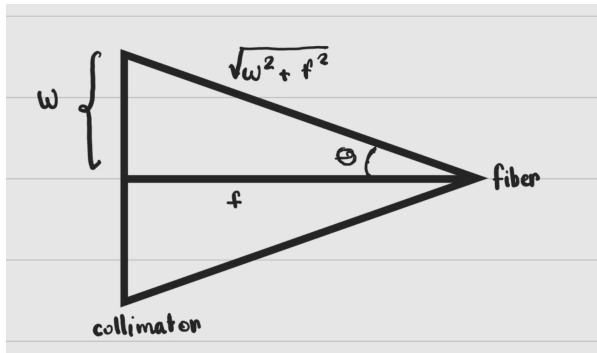


FIG. 9: The target beam waist on the collimator using NA of the fiber and the focal length of the collimator

The diameter of the collimator can be used to find the theoretical optical coupling efficiency.

$$\text{coupling efficiency: } \left(\frac{\text{NA}_{\text{fiber}}}{\text{NA}_{\text{lens}}} \right)^2$$

$$\text{NA}_{\text{lens}} = n \frac{d}{2f}$$

Appendix B: Simulation of the optical systems by Gaussian beam propagation

The following defined function is a Python program with the composite matrix system as seen in Eqn 5 for a two-lens system to propagate a beam.

```
f1 = 10 #cm #first lens focal length
f2 = 5 #cm #second lens focal length
w0 = 0.063 #cm #input laser beam waist
lamb = 633*10**-7 #cm #laser wavelength

def prep_telescope(w_0, L_a, L_b, Path):
    q0_inverse = - 1j*lamb/(np.pi*w_0**2)
    L_c = (Path) - (L_a + L_b)

    before_ABCD = np.array([[1,L_a],[0,1]])
    lens1_ABCD = np.array([[1,0],[-1/(f1),1]])
    between_ABCD = np.array([[1,L_b],[0,1]]))
```

```
lens2_ABCD = np.array([[1,0],[-1/(f2),1]])
after_ABCD = np.array([[1,L_c],[0,1]])

total_ABCD = (
    after_ABCD @ lens2_ABCD \\
    @ between_ABCD @ lens1_ABCD \\
    @ before_ABCD
)

A = total_ABCD[0][0]
B = total_ABCD[0][1]
C = total_ABCD[1][0]
D = total_ABCD[1][1]

q1_inverse = (
    (C+D*q0_inverse)/(A+B*q0_inverse))
real = np.abs(np.real(q1_inverse))
imag = np.abs(np.imag(q1_inverse))
R_1 = 1/real
w_1 = np.sqrt(1/imag*lamb*np.pi)

return R_1, w_1
```

1. Minimising Beam-waist for a collimator

The previously defined function is called and placed between constraints to find the best configurations of L_a and L_b to minimize the beam waist into the collimator. The beam waist on the collimator has been calculated in ?? from the numerical aperture of the fiber and the focal length of the collimator

```
NA = 0.12
f = 0.783 #cm
w_1 = NA*f
Total_1 = 61 #cm

result = []
min_store = []
w_threshold = []

L_a = np.linspace(0, 15, 4)
L_b = np.linspace(0, 35.8, 40)

for i in range(L_b.size):
    for j in range(L_tel.size):
        R_o, w_o = prep_telescope(0.063, L_a[i], L_b[j])
        min_store.append(abs(w_1-w_o))
        w_threshold.append([w_1, w_o, abs(w_1-w_o)])
        result.append([L_b[i], L_tel[j]])

z = np.argmin(min_store)
print ('ideal config', result[z])
print ('beam waists', w_threshold[z])
```

2. Mode-Matching a cavity at the lowest mode

A function is made for the cavity with a set-up to solve for the resonant q-parameter.

```
L = 7.62 #cm #length
B = 15.24 #cm #breadth
Diag = np.sqrt(L**2 + B**2) #cm
F = 50 #cm #CCM focal length

def prep_cavity_matching(l, f, b):
    lamb = 633*10**-7 #cm
    D = np.sqrt(l**2 + b**2)
    FreeSpaceInp_CCM = np.array([[1,l+D],[0,1]])
    CCMirror = np.array([[1,0], [-1/f, 1]])
    FreeSpaceCCM_Inp = np.array([[1, D+l],[0,1]])

    total_ABCD = (FreeSpaceCCM_Inp
    @ CCMirror @ FreeSpaceInp_CCM)

    A = total_ABCD[0][0]
    B = total_ABCD[0][1]
    C = total_ABCD[1][0]
    D = total_ABCD[1][1]

    stability = 1/4*(A+D)**2
    if stability > 1 or stability < 0:
        print ('ALERT ALERT UNSTABLE CAVITY')

    q_resonance = ((D-A/(2*B))
    - 1j*(np.sqrt(4-(A+D)**2)/(2*B)))

    real = np.abs(np.real(q_resonance))
    imag = np.abs(np.imag(q_resonance))
    R_1 = 1/real
    w_1 = np.sqrt(1/imag*lamb/np.pi)
```

```
return R_1, w_1
```

This function and the function for the telescope are used to create optimizations for the lens locations similar to the optical fiber case.

```
R_match, w_match = prep_cavity_matching(L, F, B)

Total_2 = 102.4
result = []
store_diff = []

L_a = np.linspace(0, 32, 40)
L_b = np.linspace (0, 46-32, 40)

for i in range(L_b.size):
    for j in range(L_tel.size):
        R_o, w_o = prep_telescope(0.063, L_a[i], L_b[j])
        store_diff.append([abs(w_match-w_o)])
    result.append([L_a[i], L_b[j]])

z = np.argmin(store_diff)
print ('ideal config', result[z])
```

REFERENCES

- [1] Edmund. Knuth: *Computers and Typesetting*. URL: <https://www.edmundoptics.com/knowledge-center/application-notes/lasers/gaussian-beam-propagation/>. (accessed: 11.20.2023).
- [2] UC San Diego. Knuth: *Computers and Typesetting*. URL: http://cem01.ucsd.edu/courses/ece182/182-06_files/6FiberAttenuation.pdf. (accessed: 11.20.2023).
- [3] Caltech. Knuth: *Computers and Typesetting*. URL: <http://pmaweb.caltech.edu/~ph77/labs/optics/cavities1.pdf>. (accessed: 11.20.2023).